The Journal of Chemical Physics

RESEARCH ARTICLE | DECEMBER 30 2022

Diffusion theory of molecular liquids in the energy representation and application to solvation dynamics

Kazuya Okita ; Kento Kasahara ; Nobuyuki Matubayasi

J. Chem. Phys. 157, 244505 (2022)
https://doi.org/10.1063/5.0125432

AIP Publishing

The Journal of Chemical Physics ARTICLE scitation.org/journal/jcp

Diffusion theory of molecular liquids in the energy representation and application to solvation dynamics

Cite as: J. Chem. Phys. 157, 244505 (2022); doi: 10.1063/5.0125432
Submitted: 12 September 2022 • Accepted: 28 November 2022 •
Published Online: 30 December 2022

Kazuya Okita, Kento Kasahara,[a] and Nobuyuki Matubayasi[b]

AFFILIATIONS

Division of Chemical Engineering, Graduate School of Engineering Science, Osaka University, Toyonaka, Osaka 560-8531, Japan

[a]Author to whom correspondence should be addressed: kasahara@cheng.es.osaka-u.ac.jp
[b]Electronic mail: nobuyuki@cheng.es.osaka-u.ac.jp

ABSTRACT

The generalized Langevin equation (GLE) formalism is a useful theoretical fundament for analyzing dynamical phenomena rigorously. Despite the systematic formulation of dynamics theories with practical approximations, however, the applicability of GLE-based methods is still limited to simple polyatomic liquids due to the approximate treatment of molecular orientations involved in the static molecular liquid theory. Here, we propose an exact framework of dynamics based on the GLE formalism incorporating the energy representation theory of solution, an alternative static molecular liquid theory. A fundamental idea is the projection of the relative positions and orientations of solvents around a solute onto the solute–solvent interaction, namely the energy coordinate, enabling us to describe the dynamics on a one-dimensional coordinate. Introducing systematic approximations, such as the overdamped limit, leads to the molecular diffusion equation in the energy representation that is described in terms of the distribution function of solvents on the energy coordinate and the diffusion coefficients. The present theory is applied to the solvation dynamics triggered by the photoexcitation of benzonitrile. The long-time behavior of the solvation time correlation function is in good agreement with that obtained by the molecular dynamics simulation.

I. INTRODUCTION

Molecular motions in a condensed phase are essential in various dynamic processes. Such dynamics are often characterized by sophisticated spectroscopy techniques.[1,2] For instance, time-resolved fluorescence spectroscopy can be useful to probe the solvation dynamics with a certain dye (solute), i.e., the solvent relaxation around a solute induced by the photoexcitation.[3–5] Recently, this spectroscopy has been extensively utilized to investigate the dynamics in heterogeneous environments such as the surface of biological lipid bilayers.[6,7] In its measurement, however, since the information on the dynamics is contracted to the time development of the fluorescence wavenumber, it is challenging to get the atomistic insights directly. Thus, developing a theoretical fundament to analyze the dynamics in heterogeneous environments from an atomistic point of view would be useful for further understanding.

A theoretical approach to describing the dynamics in solutions is based on transport equations, such as the Smoluchowski equation, in which the dynamics is characterized by diffusive motion and drift motion governed by the free energy gradient.[8–10] The Smoluchowski–Vlasov (SV) equation is an extension of the original Smoluchowski equation to describe the collective motion of solvents, which is a crucial part of solvation dynamics.[11–14] The molecular mode-coupling theories were also proposed to describe the dynamics of supercooled liquids.[15–17] However, these equations are useful only for simple liquids such as monoatomic and diatomic liquids because the difficulties in handling both the translational and rotational motions (six-dimensional in total) arise in the case of molecular liquids.

A route to describing such motions while avoiding the difficulty is to introduce the interaction site representation of the statistical mechanics of solution.[18,19] In its representation, the static liquid structure is expressed with a set of radial distribution functions (RDFs) between the atomic sites in molecules, realizing the effective treatment of a molecular shape and orientation. The theoretical framework for the RDFs is provided by reference interaction site

model (RISM) theory, an integral equation (IE) theory of molecular liquids,[20–23] and its extension toward the dynamic processes is achieved with Zwanzig–Mori projection operator theory.[24–28] According to this approach, the site–site Smoluchowski–Vlasov (SSSV) equation[28] and several types of site–site generalized Langevin equations (SSGLE) have been derived[29–32] and applied to various dynamic processes, such as collective excitation,[33] pressure dependence of solvent diffusivity,[34–36] electrical conduction,[37,38] ultrasound absorption,[39,40] and solvation dynamics.[41–47] Upgrading the description of the dynamics from the radial coordinate to the spatial coordinate using three-dimensional RISM (3D-RISM) theory[48–50] and the time-dependent density functional theory (TDDFT)[5,51] is a recent progress in the IE-based dynamics theories.[52–54] Thanks to the analytical nature of the theories, the developed theories are free from the sampling problems that appear in molecular dynamics (MD) simulations, and the computational cost is low. However, the applicability of the theories is still limited to simple polyatomic solvents due to the orientational averaging imposed on the solvent molecules.

Another progress in the field of the statistical mechanics of solution is the development of the energy representation (ER) theory.[55–58] Instead of the spatial coordinates, ER theory employs the interaction energy between a solute and solvent molecule as a coordinate, namely energy coordinate, for treating the relative position and orientation for molecules. It corresponds to the reduction of the dimensions required for the atomistic description from six dimensions (6D) to one dimension (1D). As well as in the case of the spatial coordinate, the Ornstein–Zernike (OZ) equation and the relationship between the density correlations and the solvation free energy can be constructed on the energy coordinate. In ER theory, once we evaluate such density correlations through MD simulations, the accurate calculation of the solvation free energy of a solute is realized.[56,59,60] Thanks to the reduction of the dimensions, the calculation of the density correlations on the energy coordinate is much easier than those in 6D space. A remarkable point of ER theory is its applicability to heterogeneous systems.[60,61] In the case of the binding of small solutes in a lipid membrane, for example, the lipid can be regarded as part of the mixed solvents.[62,63] Very recently, a diffusion-influenced reaction theory incorporating the energy coordinate was proposed to quantify the rate constants of host–guest binding processes, and its application to the binding processes of aspirin and 1-butanol to β-cyclodextrin yielded the rate constants consistent with the experimental results.[64] Accordingly, the energy coordinate would also be useful for describing dynamic processes at the atomistic scale. Furthermore, since the mathematical form of the equations derived in the framework of ER theory is almost parallel to that for the IE theory on the spatial coordinates of full 6D, position, and orientation, such as the OZ equation, the ideas of the existing IE-based dynamics theories mentioned in the last paragraph could be imported into the ER framework.

In the present study, we develop a theoretical framework for elucidating the dynamics in condensed phases by utilizing the energy coordinate. According to Zwanzig–Mori projection operator method and ER theory, an energy representation of the generalized Langevin equation (GLE) is derived. Introducing the systematic approximations such as the overdamped limit yields the energy representation of the SV (ERSV) equation by generalizing the scheme of deriving the Smoluchowski equation for molecular liquids.[65] The ERSV equation provides the solute–solvent dynamics as outputs from the static solute–solvent distribution and the diffusion coefficient as inputs. Those inputs can be readily obtained in molecular simulations, and ERSV offers a scheme for approaching the (long-time) dynamics by combining MD and GLE. We show that the solvation dynamics can be described by ERSV equation in conjunction with the linear response theory. The present theory is applied to the solvation dynamics of solvent water induced by the photoexcitation of benzonitrile.

II. THEORY

A. Ornstein–Zernike equation in the energy representation

In this subsection, we describe a brief summary of the Ornstein–Zernike (OZ) equation formalism in the energy representation.[55–57] Let us consider a system containing a solute molecule u immersed in a solvent. We regard the solute u as the source of an external field, and the position is defined as the origin of the system. We denote the full-phase space coordinate of the ith molecule of the solvent v with respect to u as $\boldsymbol{x}_{v,i}$, which refers collectively to the coordinates of the center of mass (CoM) and the orientation of the ith solvent molecule. If the solvent molecule is flexible, the intramolecular degrees of freedom are also incorporated in $\boldsymbol{x}_{v,i}$. The instantaneous distribution of solvent v in the energy representation is defined as

$$\rho_v(\varepsilon) \equiv \sum_{i\in v}\delta(\varepsilon - \varepsilon_v(\boldsymbol{x}_{v,i})), \tag{1}$$

and its fluctuation around the equilibrium average is

$$\delta\rho_v(\varepsilon) \equiv \rho_v(\varepsilon) - \langle\rho_v(\varepsilon)\rangle, \tag{2}$$

where $\langle\cdots\rangle$ stands for the ensemble average and ε_v is the defining potential between solute u and solvent v, which defines the energy coordinate, ε. Note that the defining potential, ε_v, is not limited to the solute–solvent interaction and can be defined arbitrarily depending on the phenomena of interest. It should also be noted that either the solute or solvent species are not assumed to be rigid. Moreover, the solute molecule is actually not necessary to be located at fixed position and/or orientation. The distribution of Eq. (1) can be constructed at any snapshot configuration of the solute and solvent by referring only to the value of the defining potential $\varepsilon_v(\boldsymbol{x}_{v,i})$. The density–density correlation function between solvent species v and w on the energy coordinate $\chi_{vw}(\varepsilon,\eta)$ is written as

$$\begin{aligned}\chi_{vw}(\varepsilon,\eta) &\equiv \langle\delta\rho_v(\varepsilon)\delta\rho_w(\eta)\rangle \\ &= \langle\rho_v(\varepsilon)\rangle\langle\rho_w(\eta)\rangle h_{vw}(\varepsilon,\eta) + \delta_{vw}\delta(\varepsilon-\eta)\langle\rho_v(\varepsilon)\rangle,\end{aligned} \tag{3}$$

where $h_{vw}(\varepsilon,\eta)$ is the total correlation function defined as

$$h_{vw}(\varepsilon,\eta) \equiv \frac{\langle\rho_v(\varepsilon)\rho_w(\eta)\rangle - \delta_{vw}\delta(\varepsilon-\eta)\langle\rho_v(\varepsilon)\rangle}{\langle\rho_v(\varepsilon)\rangle\langle\rho_w(\eta)\rangle} - 1. \tag{4}$$

The OZ equation in the energy representation is given as follows:

$$h_{vw}(\varepsilon,\eta) = c_{vw}(\varepsilon,\eta) + \sum_{v'} \int \mathrm{d}\zeta\ c_{vv'}(\varepsilon,\zeta)\langle\rho_{v'}(\zeta)\rangle h_{v'w}(\zeta,\eta). \tag{5}$$

Here, $c_{vw}(\varepsilon,\eta)$ is the direct correlation function, which can be related with the inverse of $\chi_{vw}(\varepsilon,\eta)$ as

$$\chi^{-1}_{vw}(\varepsilon,\eta) = \frac{\delta_{vw}}{\langle\rho_v(\varepsilon)\rangle}\delta(\varepsilon-\eta) - c_{vw}(\varepsilon,\eta). \tag{6}$$

Note that $\chi^{-1}_{vw}(\varepsilon,\eta)$ is a key quantity for constructing the dynamics theory based on the generalized Langevin equation (GLE) formalism. The numerical computation of $\chi^{-1}_{vw}(\varepsilon,\eta)$ can be performed from $\langle\rho_v(\varepsilon)\rangle$ and $\chi_{vw}(\varepsilon,\eta)$ with the aid of Moore–Penrose pseudo-inverse method when the ensemble is *NVT* or *NPT* and the number of particles in the system is invariant. The inverse matrix obtained from this method contains an additive constant. This constant is determined so as to assure the intensive property of solvation free energy in the ER theory.[57,58] As shown in Subsection II B, since the derivative of $\chi^{-1}_{vw}(\varepsilon,\eta)$ affects the dynamics, the additive constant does not contribute to the time development of the system.[57,58]

B. Diffusion equation in the energy representation

We derive a diffusion equation in the energy representation. The starting point of the derivation is the GLE formalism based on the Zwanzig–Mori projection operator method. We choose a set of the time-dependent density fluctuation, $\{\delta\rho_v(\varepsilon,t)\}$ defined below, as the dynamical variable $\boldsymbol{A}(\varepsilon,t)$

$$\boldsymbol{A}(\varepsilon,t) \equiv \begin{pmatrix} \delta\rho_1(\varepsilon,t) \\ \delta\rho_2(\varepsilon,t) \\ \vdots \end{pmatrix}, \tag{7}$$

$$\delta\rho_v(\varepsilon,t) \equiv \sum_i \delta(\varepsilon - \varepsilon_v(\boldsymbol{x}_{v,i}(t))) - \langle\rho_v(\varepsilon)\rangle. \tag{8}$$

Hereafter, the functions which do not contain time t as their arguments represent the values at $t = 0$. Performing the time derivative of $\delta\rho_v(\varepsilon,t)$ yields the continuity equation as

$$\frac{\partial\delta\rho_v(\varepsilon,t)}{\partial t} = -\frac{\partial}{\partial\varepsilon} j_v(\varepsilon,t), \tag{9}$$

where $j_v(\varepsilon,t)$ is the current field on the energy coordinate given by

$$j_v(\varepsilon,t) = \sum_i \dot{\varepsilon}_v(\boldsymbol{x}_{v,i}(t))\delta(\varepsilon - \varepsilon_v(\boldsymbol{x}_{v,i}(t))). \tag{10}$$

Let us introduce an operator $\mathcal{P}$ projecting dynamical variables onto the subspace spanned by $\boldsymbol{A}(\varepsilon)$ defined as

$$\mathcal{P}\boldsymbol{X}(\varepsilon,t) \equiv \int \mathrm{d}\eta\mathrm{d}\zeta\ \Big\langle \boldsymbol{X}(\varepsilon,t)\boldsymbol{A}^\dagger(\eta)\Big\rangle \Big\langle \boldsymbol{A}(\eta)\boldsymbol{A}^\dagger(\zeta)\Big\rangle^{-1}\boldsymbol{A}(\zeta), \tag{11}$$

where † means the adjoint. According to the standard procedure of the Zwanzig–Mori projection operator method, the following GLE in the energy coordinate is derived:

$$\frac{\partial\delta\rho_v(\varepsilon,t)}{\partial t} = -\sum_w \int_0^t \mathrm{d}\tau \int \mathrm{d}\eta\ K_{vw}(\varepsilon,\eta,\tau)\delta\rho_w(\eta,t-\tau) + F_v(\varepsilon,t). \tag{12}$$

Here, $K_{vw}(\varepsilon,\eta,t)$ and $F_v(\varepsilon,t)$ are the memory function and the fluctuating force, respectively. $F_v(\varepsilon,t)$ is defined as

$$F_v(\varepsilon,t) \equiv \exp[\mathcal{Q}i\mathcal{L}t]\mathcal{Q}i\mathcal{L}\delta\rho_v(\varepsilon) = -\exp[\mathcal{Q}i\mathcal{L}t]\frac{\partial j_v(\varepsilon)}{\partial\varepsilon}, \tag{13}$$

where $\mathcal{L}$ is the Liouville operator of the system and $\mathcal{Q}$ is the orthogonal operator defined as $\mathcal{Q} \equiv 1 - \mathcal{P}$. The memory function, $K_{vw}(\varepsilon,\eta,t)$, is represented with $F_v(\varepsilon,t)$ as follows:

$$\begin{aligned} K_{vw}(\varepsilon,\eta,t) &\equiv \sum_{v'} \int \mathrm{d}\zeta\ \langle F_v(\varepsilon,t)F_{v'}(\zeta)\rangle\chi^{-1}_{v'w}(\zeta,\eta) \\ &= \sum_{v'} \int \mathrm{d}\zeta\ \left\langle \left\{\exp[\mathcal{Q}i\mathcal{L}t]\frac{\partial j_v(\varepsilon)}{\partial\varepsilon}\right\}\frac{\partial j_{v'}(\zeta)}{\partial\zeta}\right\rangle\chi^{-1}_{v'w}(\zeta,\eta). \end{aligned} \tag{14}$$

A route for deriving the diffusion equation from the projection operator method is to replace the orthogonal time evolution operator $\exp[\mathcal{Q}i\mathcal{L}t]$ involved in Eq. (14) by the usual time evolution operator $\exp[i\mathcal{L}t]$,[65–67] corresponding to

$$F_v(\varepsilon,t) \simeq -\frac{\partial j_v(\varepsilon,t)}{\partial\varepsilon}, \tag{15}$$

where we have used Eq. (13) with the relationship given by $\exp[i\mathcal{L}t]A = A(t)$ that holds for arbitrary functions over the phase space. This approximation leads to

$$K_{vw}(\varepsilon,\eta,t) = \sum_{v'} \int \mathrm{d}\zeta\ \frac{\partial^2\langle j_v(\varepsilon,t)j_{v'}(\zeta)\rangle}{\partial\varepsilon\partial\zeta}\chi^{-1}_{v'w}(\zeta,\eta). \tag{16}$$

Similar to conventional diffusion theory, we introduce the overdamped approximation expressed in the energy representation as

$$\langle j_v(\varepsilon,t)j_w(\eta)\rangle \simeq 2\delta_{vw}\delta(\varepsilon-\eta)\delta(t)D^e_v(\varepsilon)\langle\rho_v(\varepsilon)\rangle, \tag{17}$$

where $D^e_v(\varepsilon)$ is the diffusion coefficient over the energy coordinate defined as

$$\begin{aligned} D^e_v(\varepsilon) &\equiv \frac{1}{\langle\rho_v(\varepsilon)\rangle}\int_0^\infty \mathrm{d}t \int \mathrm{d}\eta\ \langle j_v(\varepsilon,t)j_v(\eta)\rangle \\ &= \frac{1}{\langle\rho_v(\varepsilon)\rangle}\int_0^\infty \mathrm{d}t\ \langle j_v(\varepsilon,t)\dot{E}_v\rangle, \end{aligned} \tag{18}$$

where $E_v(t)$ is the sum of the defining potential between the solute and the solvent v defined as

$$E_v(t) = \sum_{i\in v}\varepsilon_v(\boldsymbol{x}_{v,i}(t)). \tag{19}$$

Using the above approximation, Eq. (16) can be rewritten as

$$K_{vw}(\varepsilon,\eta,t) = -2\delta(t)\frac{\partial}{\partial\varepsilon}\left[D_v^e(\varepsilon)\langle\rho_v(\varepsilon)\rangle\frac{\partial\chi_{vw}^{-1}(\varepsilon,\eta)}{\partial\varepsilon}\right]. \quad (20)$$

Substituting Eqs. (6) and (20) into Eq. (12) yields the following diffusion equation:

$$\frac{\partial\delta\rho_v(\varepsilon,t)}{\partial t} = \frac{\partial}{\partial\varepsilon}\left[D_v^e(\varepsilon)\frac{\partial\delta\rho_v(\varepsilon,t)}{\partial\varepsilon} - D_v^e(\varepsilon)\frac{\mathrm{d}\ln\langle\rho_v(\varepsilon)\rangle}{\mathrm{d}\varepsilon}\delta\rho_v(\varepsilon,t) - D_v^e(\varepsilon)\langle\rho_v(\varepsilon)\rangle\sum_w\int\mathrm{d}\eta\,\frac{\partial c_{vw}(\varepsilon,\eta)}{\partial\varepsilon}\delta\rho_w(\eta,t)\right] + F_v(\varepsilon,t). \quad (21)$$

The first and second terms in the square bracket, respectively, indicate the diffusive motions caused by the energy distribution gradient and the drift motions caused by the free energy gradient over the energy coordinate. The third term describes the collective motions of the solvents. Since the mathematical form of Eq. (21) is parallel to that of the Smoluchowski–Vlasov (SV) equation on the spatial coordinate proposed by Calef *et al.*,[11,14] this equation can be regarded as the energy-represented SV (ERSV) equation. The diffusive and drift terms in Eq. (21) could be combined as follows:

$$\frac{\partial\delta\rho_v(\varepsilon,t)}{\partial t} = \frac{\partial}{\partial\varepsilon}\left[D_v^e(\varepsilon)\langle\rho_v(\varepsilon)\rangle\frac{\partial}{\partial\varepsilon}\left(\frac{\delta\rho_v(\varepsilon,t)}{\langle\rho_v(\varepsilon)\rangle}\right) - D_v^e(\varepsilon)\langle\rho_v(\varepsilon)\rangle\sum_w\int\mathrm{d}\eta\,\frac{\partial c_{vw}(\varepsilon,\eta)}{\partial\varepsilon}\delta\rho_w(\eta,t)\right] + F_v(\varepsilon,t), \quad (22)$$

indicating that the time evolution of the energy distribution is governed by $D_v^e(\varepsilon)\langle\rho_v(\varepsilon)\rangle$ instead of $D_v^e(\varepsilon)$. If we neglect the third term in the square bracket, Eq. (21) is reduced to the energy-represented Smoluchowski (ERS) equation written as

$$\frac{\partial\delta\rho_v(\varepsilon,t)}{\partial t} = \frac{\partial}{\partial\varepsilon}\left[D_v^e(\varepsilon)\frac{\partial\delta\rho_v(\varepsilon,t)}{\partial\varepsilon} - D_v^e(\varepsilon)\frac{\mathrm{d}\ln\langle\rho_v(\varepsilon)\rangle}{\mathrm{d}\varepsilon}\delta\rho_v(\varepsilon,t)\right] + F_v(\varepsilon,t). \quad (23)$$

Similar to the case of the spatial coordinate,[26] the van Hove correlation function in the energy representation can be defined as follows:

$$G_{vw}(\varepsilon,\eta,t) \equiv \langle\delta\rho_v(\varepsilon,t)\delta\rho_w(\eta)\rangle. \quad (24)$$

From Eq. (21) and the orthogonality between $F_v(\varepsilon,t)$ and $\delta\rho_v(\varepsilon)$, we can obtain the differential equation for $G_{vw}(\varepsilon,\eta,t)$ as

$$\frac{\partial G_{vw}(\varepsilon,\eta,t)}{\partial t} = \frac{\partial}{\partial\varepsilon}\left[D_v^e(\varepsilon)\frac{\partial G_{vw}(\varepsilon,\eta,t)}{\partial\varepsilon} - D_v^e(\varepsilon)\frac{\mathrm{d}\ln\langle\rho_v(\varepsilon)\rangle}{\mathrm{d}\varepsilon}G_{vw}(\varepsilon,\eta,t) - D_v^e(\varepsilon)\langle\rho_v(\varepsilon)\rangle\sum_{v'}\int\mathrm{d}\zeta\,\frac{\partial c_{vv'}(\varepsilon,\zeta)}{\partial\varepsilon}G_{v'w}(\zeta,\eta,t)\right]. \quad (25)$$

C. Approximate expression of the diffusion coefficient $D_v^e(\varepsilon)$

The explicit formula of the diffusion coefficient in the energy representation is already available [Eq. (18)], which requires the energy–time correlation function, $\langle j_v(\varepsilon,t)j_v(\eta)\rangle$. In this subsection, we derive a tractable expression of $D_v^e(\varepsilon)$. Substituting Eq. (10) into Eq. (18) yields

$$D_v^e(\varepsilon) = \frac{1}{\langle\rho_v(\varepsilon)\rangle}\sum_{i,j\in v}\int_0^\infty\mathrm{d}t \times\langle\dot{\varepsilon}_v(\boldsymbol{x}_{v,i}(t))\dot{\varepsilon}_v(\boldsymbol{x}_{v,j})\delta(\varepsilon-\varepsilon_v(\boldsymbol{x}_{v,i}(t)))\rangle. \quad (26)$$

We assume that the solute molecule is located in a fixed position and orientation. Then, by expressing the full coordinate $\boldsymbol{x}_{v,i}(t)$ as a set of the positions of atoms μ in the molecule, $\boldsymbol{r}_{i,\mu}$, $\dot{\varepsilon}_v(\boldsymbol{x}_{v,i}(t))$ can be written as

$$\dot{\varepsilon}_v(\boldsymbol{x}_{v,i}(t)) = -\sum_{\mu\in i}\boldsymbol{v}_{i,\mu}(t)\cdot\boldsymbol{f}_{i,\mu}(t) = -\sum_{\mu\in i}\sum_{\alpha=x,y,z}v_{i,\mu}^\alpha(t)f_{i,\mu}^\alpha(t). \quad (27)$$

Here, $v_{i,\mu}^\alpha(t)$ is the velocity of atom μ in the ith molecule, and $f_{i,\mu}^\alpha(t)$ is the "force" corresponding to the defining potential, that is introduced as

$$\boldsymbol{f}_{i,\mu}(t) = -\frac{\partial\varepsilon_v(\boldsymbol{x}_{v,i}(t))}{\partial\boldsymbol{r}_{i,\mu}}. \quad (28)$$

If the defining potential ε_v is the same as the solute–solvent interaction, $\boldsymbol{f}_{i,\mu}(t)$ corresponds to the force acting on atom μ due to the solute–solvent interaction. In Subsection II D, we treat the solvation dynamics and set ε_v to the difference in the solute–solvent interaction potential between the ground and excited states of the solute. Using Eq. (27), Eq. (26) is written as

$$D_v^e(\varepsilon) = \sum_{i,j\in v}\sum_{\mu\in i,\lambda\in j}\sum_{\alpha,\beta=x,y,z}\frac{1}{\langle\rho_v(\varepsilon)\rangle}\int_0^\infty\mathrm{d}t \times\left\langle v_{i,\mu}^\alpha(t)v_{j,\lambda}^\beta f_{i,\mu}^\alpha(t)f_{j,\lambda}^\beta\delta(\varepsilon-\varepsilon_v(\boldsymbol{x}_{v,i}(t)))\right\rangle. \quad (29)$$

By decoupling the velocity from the force and energy, Eq. (29) is written as

$$D_v^e(\varepsilon) = \sum_{i,j\in v}\sum_{\mu\in i,\lambda\in j}\sum_{\alpha,\beta=x,y,z}\frac{1}{\langle\rho_v(\varepsilon)\rangle}\int_0^\infty\mathrm{d}t \times\left\langle v_{i,\mu}^\alpha(t)v_{j,\lambda}^\beta\right\rangle\left\langle f_{i,\mu}^\alpha(t)f_{j,\lambda}^\beta\delta(\varepsilon-\varepsilon_v(\boldsymbol{x}_{v,i}(t)))\right\rangle. \quad (30)$$

Tu *et al.* revealed that the time integral of the velocity correlation function between different atomic sites is equal to the integral for the CoM,[68] i.e.,

$$\int_0^\infty \mathrm{d}t \left\langle v_{i,\mu}^\alpha(t) v_{j,\lambda}^\beta \right\rangle = \int_0^\infty \mathrm{d}t \left\langle V_i^\alpha(t) V_j^\beta \right\rangle, \tag{31}$$

where $\boldsymbol{V}(t)$ is the CoM velocity of ith molecule. It is well known that this integral gives the translational diffusion coefficient of species v, D_v, if $i = j$ and $\alpha = \beta$. Then, we introduce the following overdamped approximation:

$$\left\langle v_{i,\mu}^\alpha(t) v_{j,\lambda}^\beta \right\rangle \simeq 2D_v \delta_{\alpha\beta}\delta_{ij}\delta(t). \tag{32}$$

It should be noted that a similar type of approximation is utilized for deriving the SSSV equation.[28] Substitution of Eq. (32) into Eq. (30) gives

$$D_v^e(\varepsilon) = \frac{1}{\langle \rho_v(\varepsilon)\rangle} D_v \sum_i \left\langle \left|\boldsymbol{f}_i^G\right|^2 \delta(\varepsilon - \varepsilon_v(\boldsymbol{x}_{v,i})) \right\rangle, \tag{33}$$

where $\boldsymbol{f}_i^G$ is the force acting on the CoM of ith molecule defined as $\boldsymbol{f}_i^G \equiv \sum_\mu \boldsymbol{f}_{i,\mu}$. The scheme of computing $\boldsymbol{f}_i^G$ is provided in Appendix. As compared to Eq. (18), this formula does not require the computation of the energy–time correlation function, leading to the reduction of the computational cost for evaluating $D_v^e(\varepsilon)$. On the other hand, since the spatial diffusivity is represented by the bulk diffusion coefficient of solvents, Eq. (33) is valid only when the solute–solvent interactions are so weak that the diffusivity of the solvent is not changed drastically around the solute. In Eq. (33), the rotational diffusion does not appear explicitly due to the decoupling of velocity from force and energy and the overdamped approximation. It could cause an insufficient description of the rotational motion of the solvent, which can be important on a short timescale.

D. Application to solvation dynamics

In this subsection, we present a scheme for describing the solvation dynamics, a response of the solvation structure to a sudden change of the electronic structure of a solute due to the photoexcitation. Let us introduce the Hamiltonians of the system at the ground and excited states as $\mathcal{H}_0$ and $\mathcal{H}_1$, respectively. The difference between the Hamiltonians is defined as

$$\begin{aligned}\Delta\mathcal{H} &\equiv \mathcal{H}_1 - \mathcal{H}_0 \\ &= \sum_v \sum_{i\in v} \left\{ u_v^e(\boldsymbol{x}_{v,i}) - u_v^g(\boldsymbol{x}_{v,i}) \right\} + \Delta E_{\mathrm{solute}},\end{aligned} \tag{34}$$

where $u_v^g(\boldsymbol{x}_{v,i})$ and $u_v^e(\boldsymbol{x}_{v,i})$ are respectively the interaction potentials between a solute and solvent v at the ground and excited states. $\Delta E_{\mathrm{solute}}$ is the change in the solute intramolecular energy due to the excitation. Only the pairwise additivity of the difference of the solute–solvent interactions at the ground and excited states is assumed in Eq. (34), and the interactions themselves and solvent–solvent interactions may not be necessarily pairwise additive. We consider the following nonequilibrium processes: At $t < 0$, the system is in equilibrium in the ground state, and the system is changed to the excited state at $t = 0$. The Hamiltonian corresponding to this process is represented as

$$\mathcal{H}(t) = \mathcal{H}_0 + \Theta(t)\Delta\mathcal{H}, \tag{35}$$

where $\Theta(t)$ is the Heaviside step function. The solvation dynamics is characterized with the solvation time correlation function (STCF), $S(t)$, defined as

$$S(t) \equiv \frac{\langle \Delta\mathcal{H}(t)\rangle_{\mathrm{ne}} - \langle \Delta\mathcal{H}(\infty)\rangle_{\mathrm{ne}}}{\langle \Delta\mathcal{H}(0)\rangle_{\mathrm{ne}} - \langle \Delta\mathcal{H}(\infty)\rangle_{\mathrm{ne}}}. \tag{36}$$

Here, $\langle\cdots\rangle_{\mathrm{ne}}$ indicates the nonequilibrium average governed by Eq. (35). In the present study, we assume that the solute molecule is rigid and its electronic structure is not modulated by the solvents, i.e., $\Delta E_{\mathrm{solute}}$ is a constant during the relaxation process. Thus, by introducing the difference of the total solute–solvent interaction between the excited and ground states at time t as

$$\Delta E(t) \equiv \sum_v \sum_{i\in v} \left\{ u_v^e(\boldsymbol{x}_{v,i}(t)) - u_v^g(\boldsymbol{x}_{v,i}(t)) \right\}, \tag{37}$$

Eq. (36) is rewritten as

$$S(t) = \frac{\langle \Delta E(t)\rangle_{\mathrm{ne}} - \langle \Delta E(\infty)\rangle_{\mathrm{ne}}}{\langle \Delta E(0)\rangle_{\mathrm{ne}} - \langle \Delta E(\infty)\rangle_{\mathrm{ne}}}. \tag{38}$$

The fluctuation-dissipation theorem provides the following tractable expression of $S(t)$ in the linear-response regime:

$$S(t) = \frac{\langle \delta\Delta E(t)\delta\Delta E\rangle}{\langle \delta\Delta E\delta\Delta E\rangle}. \tag{39}$$

Here, $\langle\cdots\rangle$ denotes an ensemble average at equilibrium with the Hamiltonian $\mathcal{H}_0$ and $\delta\Delta E(t)$ is the fluctuation of $\Delta E(t)$ in the equilibrium ensemble with $\mathcal{H}_0$, $\delta\Delta E(t) = \Delta E(t) - \langle\Delta E\rangle$. Since the system is described by $\mathcal{H}_0$ until $t = 0$, $\langle\cdots\rangle$ corresponds to the average at $t = 0$. If the potential to define the energy coordinate is set to

$$\varepsilon_v(\boldsymbol{x}_{v,i}) = u_v^e(\boldsymbol{x}_{v,i}) - u_v^g(\boldsymbol{x}_{v,i}), \tag{40}$$

$\langle\Delta E(t)\rangle_{\mathrm{ne}}$ can be simply written as

$$\Delta E(t) = \sum_v \int \mathrm{d}\varepsilon\ \varepsilon \rho_v(\varepsilon, t), \tag{41}$$

$$\langle \Delta E(t)\rangle_{\mathrm{ne}} = \sum_v \int \mathrm{d}\varepsilon\ \varepsilon \langle \rho_v(\varepsilon, t)\rangle_{\mathrm{ne}}. \tag{42}$$

In the original ER theory, the energy coordinate is defined as the solute–solvent interaction for free energy calculation, and its definition is almost parallel to that in the present study; the initial state contains a phantom solute that does not interact with the solvent, and the full solute–solvent interactions are present at the final state. It indicates that the difference between these two states becomes the full solute–solvent interaction potential. Therefore, the difference in the solute–solvent interaction between the ground and

excited states [Eq. (40)] is a natural choice as the energy coordinate for solvation dynamics. In empirical models, solvation dynamics has been regarded as the dynamics along the "solvation coordinate," which is a collective coordinate of solvent molecules usually defined as the difference in total potential energy between two different states.[69,70] Unlike such a collective coordinate, the energy coordinate [Eq. (40)] refers to the difference of pairwise solute–solvent interaction.

According to the linear response theory,[4,23,71,72] the approximate relationships are given by

$$\langle \rho_v(\varepsilon,t)\rangle_{\rm ne} - \langle \rho_v(\varepsilon,\infty)\rangle_{\rm ne} = \beta\langle \delta\rho_v(\varepsilon,t)\Delta\mathcal{H}\rangle = \beta\langle \delta\rho_v(\varepsilon,t)\Delta E\rangle \tag{43}$$

and

$$\langle \delta\rho_v(\varepsilon)\delta\rho_w(\eta)\rangle = \langle \delta\rho_v(\varepsilon)\delta\rho_w(\eta)\rangle_{\rm ES}. \tag{44}$$

Here, β is the inverse temperature, and $\langle\cdots\rangle_{\rm ES}$ represents the equilibrium average at the excited state. Equation (43) is rewritten as

$$\langle \rho_v(\varepsilon,t)\rangle_{\rm ne} - \langle \rho_v(\varepsilon,\infty)\rangle_{\rm ne} = \beta\sum_w \int {\rm d}\eta\ \eta G_{vw}(\varepsilon,\eta,t) = \beta Q_v(\varepsilon,t), \tag{45}$$

where $G_{vw}(\varepsilon,\eta,t)$ is introduced by Eq. (24) and $Q_v(\varepsilon,t)$ is defined as

$$Q_v(\varepsilon,t) \equiv \sum_w \int {\rm d}\eta\ \eta G_{vw}(\varepsilon,\eta,t) = \langle \delta\rho_v(\varepsilon,t)\delta\Delta E\rangle. \tag{46}$$

From the conservation of the number of molecules in the system, the integral of $Q_v(\varepsilon,t)$ over the energy leads to

$$\int_{-\infty}^{\infty} {\rm d}\varepsilon\, Q_v(\varepsilon,t) = 0. \tag{47}$$

Since $\langle \rho_v(\varepsilon,\infty)\rangle_{\rm ne}$ is the equilibrium distribution at the excited state, $\langle \rho_v(\varepsilon)\rangle_{\rm ES}$, Eq. (45) is expressed as

$$\langle \rho_v(\varepsilon,t)\rangle_{\rm ne} = \langle \rho_v(\varepsilon)\rangle_{\rm ES} + \beta Q_v(\varepsilon,t). \tag{48}$$

An alternative expression is obtained from the equivalence of $\langle \rho_v(\varepsilon,0)\rangle_{\rm ne}$ to $\langle \rho_v(\varepsilon)\rangle$ as

$$\langle \rho_v(\varepsilon,t)\rangle_{\rm ne} = \langle \rho_v(\varepsilon)\rangle + \beta\{Q_v(\varepsilon,t) - Q_v(\varepsilon,t=0)\}. \tag{49}$$

Substituting Eqs. (42) and (45) into Eq. (38) gives

$$S(t) = \frac{\sum_v \int {\rm d}\varepsilon\ \varepsilon Q_v(\varepsilon,t)}{\sum_v \int {\rm d}\varepsilon\ \varepsilon Q_v(\varepsilon,t=0)}. \tag{50}$$

$G_{vw}(\varepsilon,\eta,t)$ in Eq. (45) evolves with time through Eq. (25). Since Eq. (25) does not contain the differential operator acting on the energy coordinate η, the differential equation for $Q_v(\varepsilon,t)$ is readily obtained as

$$\frac{\partial Q_v(\varepsilon,t)}{\partial t} = \frac{\partial}{\partial\varepsilon}\left[D_v^e(\varepsilon)\frac{\partial Q_v(\varepsilon,t)}{\partial\varepsilon} - D_v^e(\varepsilon)\frac{{\rm d}\ \ln\langle\rho_v(\varepsilon)\rangle}{{\rm d}\varepsilon}Q_v(\varepsilon,t) - D_v^e(\varepsilon)\langle\rho_v(\varepsilon)\rangle\sum_w\int {\rm d}\eta\ \frac{\partial c_{vw}(\varepsilon,\eta)}{\partial\varepsilon}Q_w(\eta,t)\right]. \tag{51}$$

It indicates that the solvation dynamics can be described on the energy coordinate by numerically solving Eq. (51). If the solvent-solvent correlations, $c_{vw}(\varepsilon,\eta)$ are weak enough, Eq. (51) reduces to

$$\frac{\partial Q_v(\varepsilon,t)}{\partial t} = \frac{\partial}{\partial\varepsilon}\left[D_v^e(\varepsilon)\frac{\partial Q_v(\varepsilon,t)}{\partial\varepsilon} - D_v^e(\varepsilon)\frac{{\rm d}\ \ln\langle\rho_v(\varepsilon)\rangle}{{\rm d}\varepsilon}Q_v(\varepsilon,t)\right]. \tag{52}$$

In Sec. II C, an approximation for $D_v^e(\varepsilon)$ has been described. Equations (51) and (52) have been derived, on the other hand, only by combining the formulation in Sec. II B and the linear-response treatment for the solvation dynamics without resorting to any approximations to $D_v^e(\varepsilon)$. The overdamped condition of Eq. (17) is a step to Eq. (51), and an approximation may be independently adopted for $D_v^e(\varepsilon)$. $\langle\rho_v(\varepsilon)\rangle$, $D_v^e(\varepsilon)$, and $c_{vw}(\varepsilon,\eta)$ are involved in Eqs. (51) and (52), and to solve these equations, $Q_v(\varepsilon,t=0)$ is also needed as the initial condition. It should be noted that $\langle\rho_v(\varepsilon)\rangle$, $D_v^e(\varepsilon)$, $c_{vw}(\varepsilon,\eta)$, and $Q_v(\varepsilon,t=0)$ can be computed from the molecular simulation of the static ($t=0$) solute–solvent system at equilibrium with the solute being at its ground state, as well as the diffusion coefficient of the bulk solvent. The direct correlation function, $c_{vw}(\varepsilon,\eta)$, can be computed from Eq. (6) using the simulation at the ground state. Hence, Eq. (51) can be a scheme to evaluate the (long-time) dynamics on the basis of readily accessible properties in molecular simulation. Note that there are three expressions of $Q_v(\varepsilon,t=0)$ in the linear response limit. From Eqs. (44) and (46), one can obtain

$$Q_v^{(1)}(\varepsilon,t=0) = \sum_w \int {\rm d}\eta\,\eta\langle\delta\rho_v(\varepsilon)\delta\rho_w(\eta)\rangle \tag{53}$$

and

$$Q_v^{(2)}(\varepsilon,t=0) = \sum_w \int {\rm d}\eta\,\eta\langle\delta\rho_v(\varepsilon)\delta\rho_w(\eta)\rangle_{\rm ES}. \tag{54}$$

Since the value of $\langle\rho_v(\varepsilon,t=0)\rangle$ is equivalent to $\langle\rho_v(\varepsilon)\rangle$, Eq. (48) is rewritten as

$$Q_v^{(3)}(\varepsilon,t=0) = \frac{1}{\beta}\{\langle\rho_v(\varepsilon)\rangle - \langle\rho_v(\varepsilon)\rangle_{\rm ES}\}. \tag{55}$$

While Eqs. (53) and (54) require molecular simulations only at the ground and excited states, respectively, simulations both at the ground and excited states are required for Eq. (55). In the present study, we utilize Eq. (53) for computing the initial value.

III. COMPUTATIONAL METHODS

A. System modeling

We investigated the aqueous solution of benzonitrile at the infinite dilution limit. The structure of benzonitrile was optimized at the MP2/6-31G(d) level calculation with Gaussian16.[73] The atomic

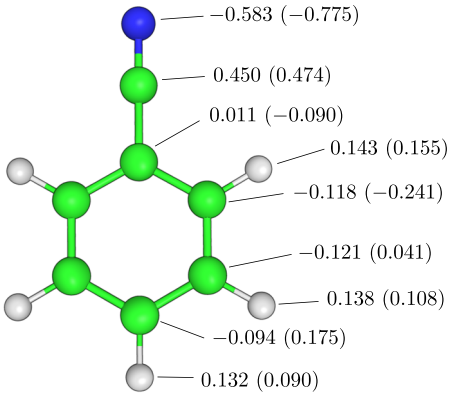

FIG. 1. Atomic point charges for benzonitrile at the ground and excited states. The values in parentheses mean the charges at the excited state. The carbon, nitrogen, and hydrogen atoms are depicted in green, blue, and gray, respectively. The absolute value of the dipole moment changes from 5.88 to 12.6 D due to the excitation.

point charges of benzonitrile at the ground and excited states were taken from the previous study by Ishida *et al.*,[44] and these values are shown in Fig. 1. The force fields for benzonitrile and water molecules are the generalized Amber force field (GAFF)[74] and TIP3P, respectively. In order to check the box size dependency of the present calculations, we prepared two systems with different box sizes, $60 \times 60 \times 60$ Å^3 (7200 water molecules) and $80 \times 80 \times 80$ Å^3 (17 067 water molecules). The schemes for MD simulations described below were adopted for both systems. The initial configurations were built using Packmol.[75]

B. Simulation setups

We performed three types of MD simulations of benzonitrile in water at 298.15 K with constant volumes and numbers of particles. One is at equilibrium with benzonitrile in its ground state, and the others are with excited-state benzonitrile. The second type is in the equilibrium condition, and the last one is the nonequilibrium MD (NEMD) simulations corresponding to the solvent relaxation process due to the photoexcitation of benzonitrile. The results from the NEMD simulations were used for comparison with those from the present theory.

To perform a series of MD simulations at equilibrium, we prepared the system configurations separately at the ground and excited states for benzonitrile. At each state, an MD simulation was performed for 1 ns. Then, we carried out the simulations for 5 ns at the ground state and for 1 ns at the excited state to extract the configurations every 1 ps. The total number of sampled configurations was 5000 and 1000 at the ground and excited states, respectively. We performed the simulations for 0.5 ns starting from the sampled configurations for equilibration, where the random seed for the thermostat was different among the distinct runs. The production MD simulations (1 ns for each) were performed at the ground and excited states, and the number of trajectories was 1000 at each state. We also conducted 5000 NEMD simulations (2 ps for each) starting from the configurations at the ground state while using the atomic charges of benzonitrile at the excited state.

For all the simulations, we used the velocity Verlet (VVER) integrator[76] with a time interval of 2 fs and the Bussi thermostat.[77] The benzonitrile molecule was treated as rigid by setting the velocities of its atoms to zero, corresponding to the neglect of both the translational and rotational motions of benzonitrile. The cutoff distance of Lennard-Jones potentials was 9.0 Å, and the smoothed particle mesh Ewald (SPME) method was used to calculate the electrostatic potential, as described in the Appendix. Water molecules were kept rigid using the SETTLE algorithm.[78] All the MD simulations were performed with GENESIS 2.0 beta,[79–81] in which the freeze scheme of a molecule was implemented by us. All the analyses were performed using in-house Fortran90/95 programs combined with the visual molecular dynamics (VMD) package (ver. 1.9.4 alpha)[82] and ERmod 0.3.7.[58]

C. Solver for ERSV and ERS equations

In order to numerically solve the ERSV and ERS equations, we constructed a scheme for treating these equations in their discretized forms. It is known that the solvent distribution on the energy coordinate has a very sharp peak around $\varepsilon = 0$. For numerical accuracy, we introduced a function for generating non-uniform grids on the energy coordinate, which are fine around $\varepsilon = 0$ (see Sec. S1 and Fig. S1 of the supplementary material). The discretization was performed with the finite volume method (FVM) to assure the conservation law of particle number, as shown in Fig. S2 of the supplementary material.[83] As well as in the case of a solver of the Smoluchowski equation,[84] the drift term was discretized by the 1st-order upwind difference scheme, and the ERSV and ERS equations were integrated by the full implicit algorithm to obtain the numerical stability. The time grid Δt was set to be 1 fs. Further details of the solver are shown in Sec. S2 of the supplementary material.

IV. RESULTS AND DISCUSSION

A. Solvent distribution on the energy coordinate

First, we examine the solvent distributions on the energy coordinate at the ground state of benzonitrile, $\langle \rho(\varepsilon) \rangle$ [Fig. 2(a)]. Hereafter (including Fig. 2), the subscript ν adopted in Sec. II is dropped for notational simplicity. The energy coordinate, ε, is defined as the difference in the solute–solvent interaction energy between the excited and ground states. Thus, the destabilized and stabilized water molecules due to the excitation contribute to the distribution at $\varepsilon > 0$ and $\varepsilon < 0$, respectively. It is seen for the benzonitrile solute at the ground state that the distribution monotonically increases with ε at $\varepsilon < 0$. When MD simulations are done with the excited-state benzonitrile, a shallow well of the distribution exists at $\varepsilon = -2.8$ kcal mol^{-1}, and the population corresponding to stabilized water molecules ($\varepsilon < 0$) is increased (see Fig. S3 of the supplementary material). The shapes of the distributions obtained from MD simulations with the different box lengths are almost the same as each other except for $\varepsilon \simeq 0$. It is well known that the energy distribution function has the system size dependency around $\varepsilon = 0$ and shows divergent behavior as the box size increases. As will be discussed in Sec. IV B, on the other hand, the system size dependency of $\langle \rho(\varepsilon) \rangle$ is canceled with that of $D^e(\varepsilon)$ for the dynamics.

The locations of stabilized and destabilized water molecules can be illustrated by computing the water CoM densities in the spatial regions corresponding to $\varepsilon \le -2.8$ kcal mol^{-1} and $\varepsilon \ge 1.5$ kcal mol^{-1},

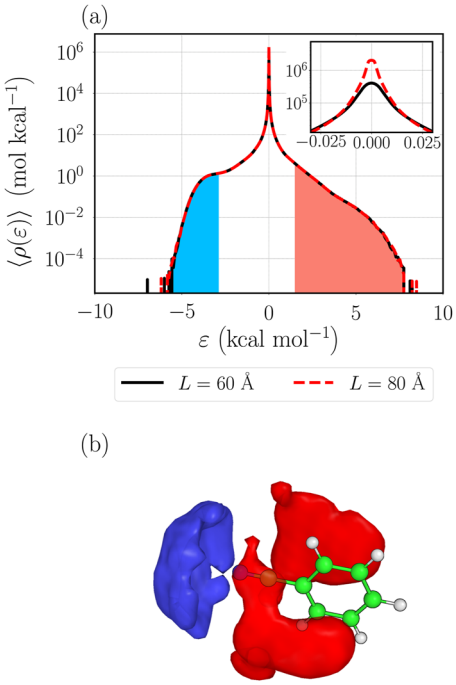

FIG. 2. Solvent distributions at the ground state. (a) The distributions on the energy coordinate obtained from simulations with different box lengths, L = 60 Å and 80 Å. The energy coordinate ε is defined as the difference between the solute–solvent interaction potential at the ground state and that at the excited state. (b) The spatial distribution function (SDFs), $g_S(\boldsymbol{r})$, corresponding to the destabilized region ($\varepsilon \geq 1.5$ kcal mol^{-1}, red) and the stabilized region ($\varepsilon \leq -2.8$ kcal mol^{-1}, blue). The $g_S(\boldsymbol{r})$ at the isovalue of 0.4 are visualized with PyMOL.[85] In (a), those regions are shaded in cyan and orange, respectively.

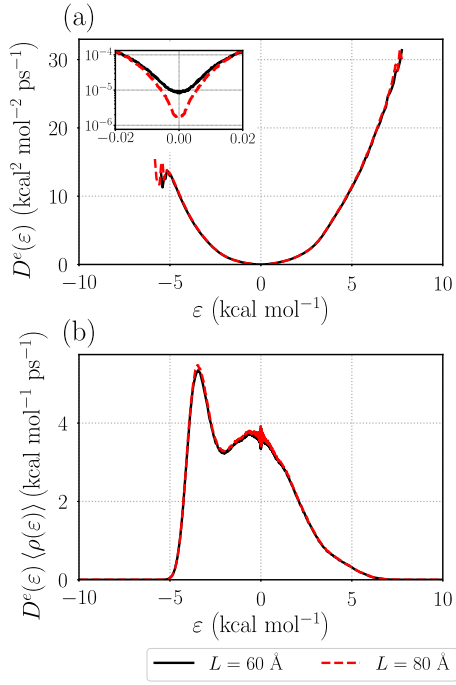

FIG. 3. Solvent diffusivity on the energy coordinate. (a) Diffusion coefficients, $D^e(\varepsilon)$, and (b) $D^e(\varepsilon)\langle\rho(\varepsilon)\rangle$.

respectively, and determining the spatial distribution functions (SDFs), $g_S(\boldsymbol{r})$, as their ratios to the bulk density of water. SDFs are shown in Fig. 2(b), and they indicate that the most stabilized water molecules are localized around the nitrogen atom of benzonitrile, while the destabilized ones are distributed around the benzene ring. The same trend is also observed in the SDFs with different isovalues [see Fig. S4(a) of the supplementary material]. The stabilized region in the excited state becomes wider than that in the ground state [see Fig. S4(b) of the supplementary material]. It can be confirmed from the radial distribution function (RDF) for the stabilized region that the stabilized water molecules dominantly contribute to the first solvation shell around the nitrogen atom (see Fig. S5 of the supplementary material). Considering the fact that the excitation makes the nitrogen charge more negative, the distribution of the stabilized water molecules is reasonable.

B. Diffusion coefficient on the energy coordinate

The diffusion coefficients on the energy coordinate, $D^e(\varepsilon)$, calculated from Eq. (33) are shown in Fig. 3(a). The minimum is located around $\varepsilon = 0$, indicating that the difference of the solute–solvent interaction between the excited and ground states varies slowly in the region. This is because the bulk water molecules are dominant around $\varepsilon = 0$, and their wandering has little contribution to the change in the energy coordinate. On the other hand, high diffusivity is observed in both the stabilized ($\varepsilon < 0$) and destabilized ($\varepsilon > 0$) regions. From the definition [Eq. (33)], $D^e(\varepsilon)$ is large when the large force acts on the solvent molecules. Therefore, the high diffusivity in the stabilized and destabilized regions can be interpreted that the difference in the solute–solvent interactions in these regions varies significantly depending on their configurations. The system size dependency is slightly discernible around $\varepsilon = 0$. As shown in Eq. (22), however, $D^e(\varepsilon)$ appears with $\langle\rho(\varepsilon)\rangle$, i.e.,

$$D^e(\varepsilon)\langle\rho(\varepsilon)\rangle = D\sum_i \left\langle \left|\boldsymbol{f}_i^G\right|^2 \delta(\varepsilon - \varepsilon(\boldsymbol{x}_i))\right\rangle, \tag{56}$$

and hence the system size dependency should be discussed with $D^e(\varepsilon)\langle\rho(\varepsilon)\rangle$ instead of $D^e(\varepsilon)$. Figure 3(b) reveals that the dependency of $D^e(\varepsilon)\langle\rho(\varepsilon)\rangle$ on the system size is negligibly small. The number of bulk molecules corresponding to region $\varepsilon \sim 0$ depends on the system size, but the force $\left|\boldsymbol{f}_i^G\right|$ for such molecules is small. Thus, they do not contribute to $D^e(\varepsilon)\langle\rho(\varepsilon)\rangle$ [Eq. (56)], leading to the cancelation of the system size dependencies appearing in $\langle\rho(\varepsilon)\rangle$ and $D^e(\varepsilon)$. The water molecules around benzonitrile, which are neither stabilized nor destabilized by the excitation, dominantly contribute to region $\varepsilon \sim 0$. According to Fig. 2, most of the water molecules, which belong to the high peak of $D^e(\varepsilon)\langle\rho(\varepsilon)\rangle$ located at ~ -3.5 kcal mol^{-1} in Fig. 3(b), coordinate to the nitrogen atom of benzonitrile. Hence, the well existing at ~ -2 kcal mol^{-1} can be interpreted as a kinetic trap for changing the states of water molecules around benzonitrile.

C. Relaxation of the solvent distribution

We discuss the time development of $\langle \rho(\varepsilon,t)\rangle_{\rm ne}$ obtained by numerically solving the ERSV equation for $Q(\varepsilon,t)$. In the computation, the initial value of $Q(\varepsilon,t)$ is evaluated through Eq. (53), i.e., $Q(\varepsilon,t=0) = Q^{(1)}(\varepsilon,t=0)$. A comparison of $Q^{(1)}(\varepsilon,t=0)$ with $Q^{(2)}(\varepsilon,t=0)$ and $Q^{(3)}(\varepsilon,t=0)$ (Fig. S6 of the supplementary material) reveals that the difference between them is sufficiently small. Note that the computed $Q_v(\varepsilon,t)$ satisfactory reproduces the conservation law [Eq. (47)], revealing the validity of the present numerical scheme (see Fig. S7 of the supplementary material). In Fig. 4, the time development of $\langle \rho(\varepsilon,t)\rangle_{\rm ne}$ using Eq. (49) is illustrated together with that from the NEMD simulations. It is seen from $\langle \rho(\varepsilon,t)\rangle_{\rm ne}$ with the ERSV equation [Fig. 4(a)] that a peak arises at ~ -3.5 kcal mol^{-1} immediately after the excitation and that its peak height becomes higher as time proceeds. A similar trend is also observed in the distribution from the NEMD simulations [Fig. 4(b)]. Although the differences in peak heights and shapes at $0.1 \le t/\text{ps} \le 0.8$ are discernible between the ERSV equation and the NEMD simulations, a good agreement is realized at $t \ge 1.0$ ps. The rate of decreasing the population in $\varepsilon > 0$ predicted from the ERSV equation is much slower compared with the NEMD simulations, suggesting the importance of the inertial and memory effects for reproducing the fast relaxation process, which are neglected in the ERSV equation. The time development of $\langle \rho(\varepsilon,t)\rangle_{\rm ne}$ using Eq. (48) is similar to that using Eq. (49) (see Fig. S8 of the supplementary material). In Fig. 4(a), an unphysical negative distribution is slightly discernible around $\varepsilon \sim 3$ kcal mol^{-1}, as also reported in the case of the spatial site distribution functions obtained by the surrogate theory.[42] Such a behavior can be interpreted as a nonlinearity of the solvation dynamics. Further discussion is found in Sec. S3 and Fig. S9 of the supplementary material. On the other hand, it should be emphasized that the negative distribution in Fig. 4(a) is negligibly small, and hence the linear response treatment is essentially valid for the present system.

For a more quantitative comparison, we analyze the change in the number of water molecules in the stabilized region ($\varepsilon \le -2.8$ kcal mol^{-1}) and in the destabilized region ($\varepsilon \ge 1.5$ kcal mol^{-1}), as shown in Fig. S10 of the supplementary material. It is found that the difference in the number of water molecules between the ERSV equation and the NEMD simulations is smaller than unity, even in the destabilized region. Hence, the prediction of the time development of $\langle \rho(\varepsilon,t)\rangle_{\rm ne}$ using ERSV equation is useful for understanding the dynamics on the long timescale in detail.

D. Solvation time correlation function

In this subsection, we address the accuracy of the solvation time correlation functions (STCFs), $S(t)$, obtained from the ERSV equation. For comparison, we also compute the function from the MD simulations at the equilibrium ground state by employing an approximate expression derived from the linear response theory, Eq. (39). Note that the approximated STCF from the MD simulations matches the exact function from the NEMD simulations with Eq. (38), proving the validity of the linear response theory for the present system (see Fig. S11 of the supplementary material). Figure 5 shows the STCFs and the time-dependent relaxation time coefficients defined as

$$\tau(t) = -\left(\frac{\mathrm{d}\ln S(t)}{\mathrm{d}t}\right)^{-1}, \tag{57}$$

obtained from the ERSV equation and from the MD simulations at the equilibrium ground state [Eq. (39)]. Note that $\tau(\infty)$ coincides with the relaxation time constant in the diffusion regime. The linear plots of the STCFs are available in Fig. S12 of the supplementary material. In order to reduce the statistical noise in $S(t)$ from the MD simulations, the moving average scheme was employed. The numbers of points for the average were 5 for $0 < t/\text{ps} < 0.5$, 21 for $0.5 < t/\text{ps} < 1.0$, and 51 for $1.0 < t/\text{ps} < 2.0$, where the time interval

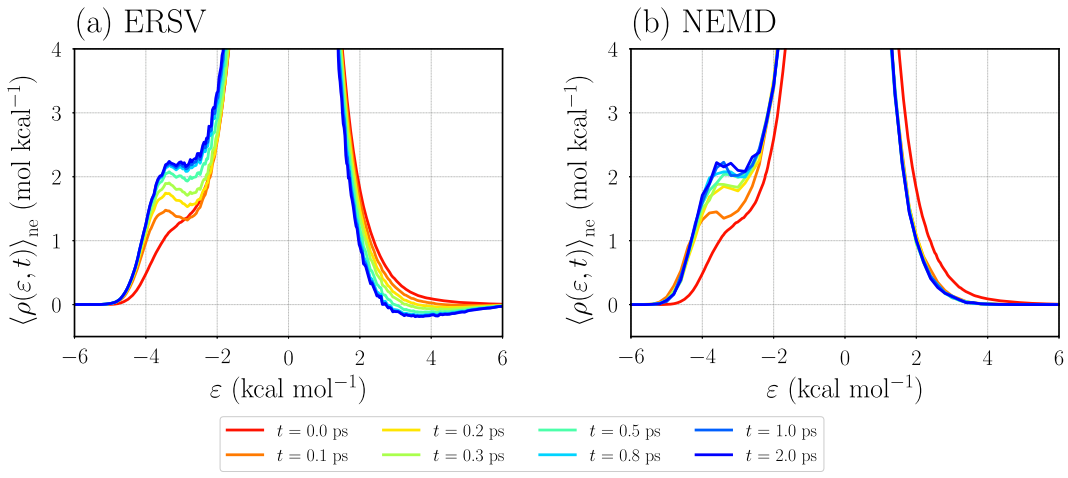

FIG. 4. Time developments of the distributions on the energy coordinate after the excitation of benzonitrile, obtained from (a) the ERSV equation and (b) NEMD simulations. In the case of ERSV equation, Eq. (49) is used for computing $\langle \rho(\varepsilon,t)\rangle_{\rm ne}$. The box length of the simulations is 60 Å for both the cases.

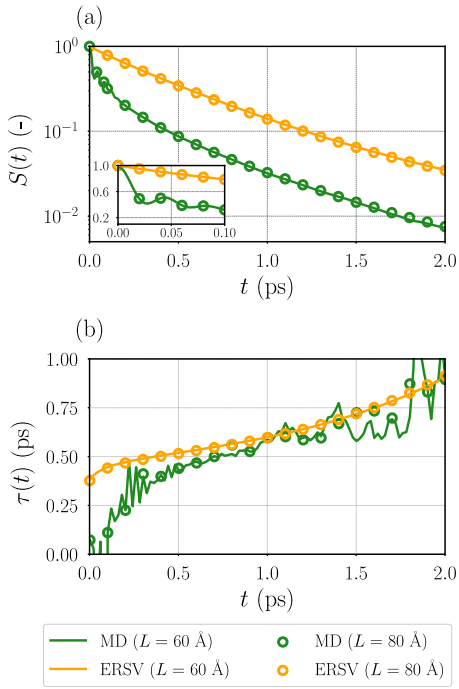

FIG. 5. Time correlation functions for the solvent relaxation process obtained from the ERSV equation and the MD simulation at the equilibrium ground state. (a) Solvation time correlation functions (STCFs), $S(t)$, and (b) time-dependent relaxation time coefficients, $\tau(t)$.

used for computing $S(t)$ is 0.002 ps. It is confirmed that this operation hardly changes the curves of $S(t)$. While $S(t)$ obtained from the ERSV equation decays monotonically, the initial Gaussian decay followed by the damped oscillation appears on a short timescale in $S(t)$ from the MD simulations (see Fig. S13 of the supplementary material). As Nishiyama *et al.* mentioned in their study using SSSV and RISM/mode-coupling theories,[47] such oscillations reflect the memory effects of solvent motions. In order to elucidate the origin of the oscillations, we computed the time correlation functions of the rotational motions of the water molecules coordinating to the nitrogen atom of benzonitrile with the hydrogen bonding from the MD simulations. The definitions of the functions are described in Sec. S4 and Fig. S14 of the supplementary material. The time correlation functions are shown in Fig. S15 of the supplementary material. The phase and frequency of the damped oscillations appearing in these functions are found to be the almost same as that in $S(t)$. Hence, the rotational motion of water molecules restricted by hydrogen bonding has a vital role in the dynamics on the short timescale. The slower decay of $S(t)$ from the ERSV equation compared with the MD simulation might stem from the insufficient description of the rotational motion in $D^e(\varepsilon)$ [Eq. (33)] in the decoupling approximation [Eq. (30)]. An upgrade of the method so as to include the memory effect and rotational motion is important for accurately describing the fast relaxation dynamics. On the other hand, although the discrepancy between the ERSV equation and the MD simulations is shown due to the difference in $S(t)$ appearing at $t \leq 0.5$ ps, the slopes of $S(t)$ on the logarithmic scale for the ERSV equation and the MD simulations are similar to each other at $t > 1.0$ ps. As also shown in Fig. 5(b), $\tau(t)$ from the ERSV equation is in accord with that from the MD simulations at $t > 0.5$ ps. It indicates that the dynamics on the long timescale is well captured by the ERSV equation (without sufficient treatments of the rotational motions). Furthermore, it should be emphasized that the present theory can be used to robustly discuss the dynamics on a long timescale while avoiding sampling error. In comparison, $\tau(t)$ obtained from MD simulations shows noise due to poor sampling, and this noise could be problematic to determine the relaxation time constant on the long timescale.

In addition to the usefulness of the present theory for describing the dynamics on a long timescale, a systematic analysis of the effect of collective solvent diffusion is available using both the ERSV and ERS equations. Since the ERS equation is derived by neglecting the collective diffusion part of the ERSV equation, only the single-particle diffusion process is taken into account in the ERS equation. Thus, it can be stated that the difference in $S(t)$ between the ERSV and ERS equations reflects the significance of collective diffusion on the relaxation process. The time developments of $S(t)$ and $\tau(t)$ computed from these equations are shown in Fig. 6. It is seen that the system size dependency of $S(t)$ is slightly apparent for the ERSV equation at $t > 20$ ps, while such a dependency is not present in the function from the ERS equation. In the case of the ERS equation, the deviation of $S(t)$ from the MD simulations is larger as compared to the ERSV equation. It is further observed that $S(t)$ decays more slowly with ERS than with ERSV, showing that the collective

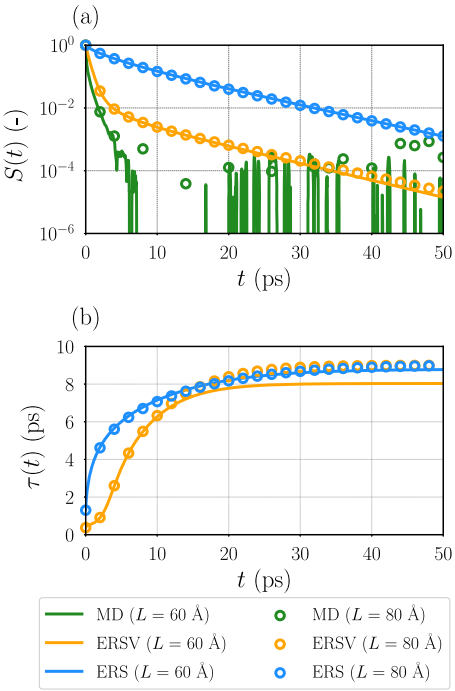

FIG. 6. Time correlation functions for the solvent relaxation process obtained from ERSV and ERS equations. (a) Solvation time correlation functions (STCFs), $S(t)$, and (b) time-dependent relaxation time coefficients. For comparison, $S(t)$ obtained from the MD simulation at the equilibrium ground state is also shown.

motion of solvent molecules facilitates the relaxation. The difference is evident on the timescale of $t < 10$ ps and still alive on the longer timescale. Interestingly, the value of $\tau(t)$ from the ERS equation becomes close to that from the ERSV equation as time proceeds, as described in Fig. 6(b). At $t > 15$ ps, the match of $\tau(t)$ with the ERSV equation is observed when the box length of the system, L, is 80 Å. Accordingly, the collective diffusion has an impact on the relaxation process until 15 ps.

V. CONCLUDING REMARKS

We formulated the energy-represented generalized Langevin equation (ERGLE), an exact differential equation, based on Zwanzig–Mori projection operator method. In the equation, the molecular motions are described over one-dimensional space without any approximations using the solute–solvent interaction energy as the coordinate. The quantities involved in ERGLE were introduced in low-dimensional coordinates compared with those employing the conventional coordinates of the positions and orientations of molecules, and hence their evaluation using the molecular dynamics (MD) simulation can be much easier. Thanks to the exact treatment of the dynamics, ERGLE would be useful for describing the dynamic processes occurring in molecular liquids composed of arbitrary complicated molecules and in heterogeneous environments, such as lipid membranes. The energy-represented Smoluchowski–Vlasov (ERSV) and Smoluchowski (ERS) equations were formulated by systematically neglecting the inertial and memory effects, which can be important for short-time dynamics. They are thus a scheme for describing the long-time dynamics and adopt the (static) solvent distribution and diffusion coefficient on the energy coordinate as inputs, which can be easily evaluated through MD simulations. It should be noted that the present theory makes no assumptions about the chemical properties of solvents and hence offers a theoretical fundament to analyze the dynamics in various solvent systems, such as protic/aprotic solvents and ionic liquids.

ERSV and ERS equations were applied to the water relaxation process triggered by the photoexcitation of benzonitrile in conjunction with the linear response theory. The solvent distribution and diffusion coefficient on the energy coordinate were examined. The energy coordinate, ε, was defined as the difference in the solute–solvent interaction energy between the excited and ground states of benzonitrile. The distribution showed the populations of stabilized and destabilized water molecules due to the excitation of benzonitrile, and these molecules were found to be localized around the nitrogen atom and benzene ring of benzonitrile, respectively. The diffusivity of water on the energy coordinate was high in the stabilized and destabilized regions on the energy coordinate, while that for the bulk water was quite small. Both the distribution and diffusion coefficients showed system-size dependencies around $\varepsilon \sim 0$, but we revealed that these dependencies brought no system-size dependency to the dynamical behavior obtained from the ERSV and ERS equations. The time development of the nonequilibrium distribution obtained from the ERSV equation showed the growth of the peak in the stabilized region, which is also observed in the nonequilibrium MD (NEMD) simulations. Although the difference in distribution between the ERSV and the NEMD simulation was discernible, especially in the destabilized region on the short timescale, a good agreement was realized on the long timescale. The solvation time correlation function (STCF) obtained from the ERSV equation deviated from that from the MD simulations due to the difference appearing on the short timescale. On the other hand, the ERSV equation reproduced the relaxation time coefficient from the MD simulations on the long timescale, indicating the usefulness of the ERSV equation for describing the long-time dynamics. The comparison of the STCF obtained from the ERS equation with that obtained from the ERSV equation clarified the impact of the collective solvent diffusion on the relaxation time. For further investigation, on the other hand, developing the methodology to realize the decomposition of $S(t)$ into the contributions of a variety of motional modes in the ER framework would be important for increasing the usefulness of the present study.

We shall comment on the possibility of improving the description of the dynamics based on the energy-represented theory. In the present study, an approximated expression of the diffusion coefficient on the energy coordinate uses the translational diffusion coefficient of water in the bulk, and this treatment should be valid only for homogeneous systems with weak solute–solvent interactions. Since the ERSV and ERS have been derived without referring to an explicit expression for the diffusion coefficient, any upgrade to the approximation for the diffusivity will lead to an improvement of the theory. The inertial and memory effects are vital for describing the short-time dynamics. As well as in the case of the theories using the spatial coordinate,[71] a formulation of the GLEs for the solvent distribution and its current might be important for treating the inertial effect. As for the memory effect, importing the approximations utilized in the viscoelastic[86,87] and mode-coupling[88–90] theories into the ER framework might be promising. We believe that further improvement would lead to a deeper understanding of the dynamical behaviors in complex molecular liquids and in heterogeneous environments.

SUPPLEMENTARY MATERIAL

The supplementary material contains the method to build a non-uniform grid energy coordinate, the numerical scheme to solve the ERSV equation, the analysis of the nonlinearity in the solvation dynamics, and additional results.

ACKNOWLEDGMENTS

This work was supported by the Grant-in-Aid for Scientific Research (Grant Nos. JP21K14589, JP22J21080) from the Japan Society for the Promotion of Science and by the Fugaku Supercomputer Project (Grant No. JPMXP1020200308) and the Elements Strategy Initiative for Catalysts and Batteries (Grant No. JPMXP0112101003) from the Ministry of Education, Culture, Sports, Science, and Technology.

VI AUTHOR DECLARATIONS

Conflict of Interest

The authors have no conflicts to disclose.

Author Contributions

Kazuya Okita: Conceptualization (supporting); Data curation (lead); Formal analysis (lead); Investigation (lead); Methodology (lead); Software (lead); Validation (lead); Visualization (lead); Writing – original draft (equal). **Kento Kasahara**: Conceptualization (lead); Data curation (lead); Formal analysis (lead); Funding acquisition (lead); Investigation (lead); Methodology (lead); Project administration (lead); Resources (lead); Software (lead); Supervision (lead); Validation (lead); Writing – original draft (equal); Writing – review & editing (equal). **Nobuyuki Matubayasi**: Conceptualization (lead); Formal analysis (supporting); Funding acquisition (lead); Investigation (supporting); Methodology (supporting); Project administration (lead); Resources (lead); Software (supporting); Supervision (lead); Validation (supporting); Writing – review & editing (equal).

DATA AVAILABILITY

The data that support the findings of this study are available from the corresponding author upon reasonable request.

APPENDIX: SCHEME OF COMPUTING PAIR ENERGY AND FORCE

To apply the present theory to molecular systems, we have to evaluate the pair interaction energy between solute (u) and solvent (v) molecules and the pair force acting on a solvent molecule due to the solute–solvent interaction. Currently, the smoothed particle mesh Ewald (SPME) proposed by Essmann *et al.* is the most widely used method to compute the electrostatic interactions of the whole system, as adopted in this work.[91] As for the pair energy, Sakuraba *et al.* derived the theoretical expression when the electrostatic interaction is treated with the SPME method.[58] In this appendix, we derive the expression of the pair force based on their derivation.

Let us define the pair energy between a solute and ith solvent molecule, u_i^{uv}, as follows:

$$u_i^{uv} = u_{\mathrm{LJ},i}^{uv} + u_{\mathrm{elec},i}^{uv}. \tag{A1}$$

Here, $u_{\mathrm{LJ},i}^{uv}$ and $u_{\mathrm{elec},i}^{uv}$ are, respectively, Lennard-Jones (LJ) and electrostatic interactions defined as

$$u_{\mathrm{LJ},i}^{uv} \equiv \sum_{\mu\in u}\sum_{\nu\in i} 4\varepsilon_{\mu\nu}\left[\left(\frac{\sigma_{\mu\nu}}{r_{\mu\nu}}\right)^{12} - \left(\frac{\sigma_{\mu\nu}}{r_{\mu\nu}}\right)^{6}\right], \tag{A2}$$

$$u_{\mathrm{elec},i}^{uv} \equiv \sum_{\mu\in u}\sum_{\nu\in i} \frac{q_\mu q_\nu}{r_{\mu\nu}}, \tag{A3}$$

where $r_{\mu\nu}$ is the distance between μ and ν atoms, $\sigma_{\mu\nu}$ and $\varepsilon_{\mu\nu}$ are the LJ parameters, and q_μ is the point charge on atom μ. The electrostatic interaction in SPME is modified from Eq. (A3) and is divided into the short-range ($u_{\mathrm{elec},i}^{(s)}$) and long-range ($u_{\mathrm{elec},i}^{(l)}$) parts as

$$u_{\mathrm{elec},i}^{uv} = u_{\mathrm{elec},i}^{(s)} + u_{\mathrm{elec},i}^{(l)}. \tag{A4}$$

$u_{\mathrm{elec},i}^{(s)}$ is given by

$$u_{\mathrm{elec},i}^{(s)} \equiv \sum_{\mu\in u}\sum_{\nu\in i} \frac{q_\mu q_\nu}{r_{\mu\nu}}(1 - \mathrm{erf}(\kappa r_{\mu\nu})), \tag{A5}$$

where $\mathrm{erf}(x)$ is the error function defined as

$$\mathrm{erf}(x) \equiv \frac{2}{\sqrt{\pi}}\int_0^x \mathrm{d}y\ \exp\left[-y^2\right], \tag{A6}$$

and κ is the screening parameter. $u_{\mathrm{LJ},i}^{uv}$ and $u_{\mathrm{elec},i}^{(s)}$ can be calculated with a simple cutoff scheme. As for $u_{\mathrm{LJ},i}^{(l)}$, the efficient computation can be performed via the reciprocal (Fourier) space thanks to the periodicity of the simulation system. In the SPME method, $u_{\mathrm{elec},i}^{(l)}$ consists of the reciprocal-space energy part ($u_{\mathrm{recp},i}$) and the correction part for neutralizing background ($u_{\mathrm{corr},i}$) as

$$u_{\mathrm{elec},i}^{(l)} = u_{\mathrm{recp},i} + u_{\mathrm{corr},i}. \tag{A7}$$

$u_{\mathrm{corr},i}$ is represented as

$$u_{\mathrm{corr},i} = -\sum_{\mu\in u}\sum_{\nu\in i} \frac{\pi q_\mu q_\nu}{\kappa^2 V}, \tag{A8}$$

where V is the system volume. The computation of $u_{\mathrm{corr},i}$ is performed with the discretized Fourier transform. Thus, we introduce the discretized spatial grids as

$$\begin{cases} x_{k_x} = k_x\Delta x, & k_x = 0, 1, \ldots, K_x, \\ y_{k_y} = k_y\Delta y, & k_y = 0, 1, \ldots, K_y, \\ z_{k_z} = k_z\Delta z, & k_z = 0, 1, \ldots, K_z, \end{cases} \tag{A9}$$

where $\Delta\alpha = L_\alpha/K_\alpha$ ($\alpha = x, y, z$), where L_α is the cell length along the α direction. The discrete Fourier transform $\mathcal{F}[\cdots]$ and inverse transform $\mathcal{F}^{-1}[\cdots]$ are defined as

$$\mathcal{F}[f](m_x, m_y, m_z) \equiv \sum_{k_x=0}^{K_x-1}\sum_{k_y=0}^{K_y-1}\sum_{k_z=0}^{K_z-1} f(k_x, k_y, k_z) \times \exp\left[-2\pi\imath\left(\frac{m_x k_x}{K_x} + \frac{m_x k_x}{K_x} + \frac{m_x k_x}{K_x}\right)\right], \tag{A10}$$

$$\mathcal{F}^{-1}[f](k_x, k_y, k_z) \equiv \sum_{m_x=0}^{K_x-1}\sum_{m_y=0}^{K_y-1}\sum_{m_z=0}^{K_z-1} f(m_x, m_y, m_z) \times \exp\left[2\pi\imath\left(\frac{m_x k_x}{K_x} + \frac{m_x k_x}{K_x} + \frac{m_x k_x}{K_x}\right)\right], \tag{A11}$$

where $\imath \equiv \sqrt{-1}$. Furthermore, we define the following atom-wise grid charge distribution of atom μ, $Q_\mu(k_x, k_y, k_z)$:

$$Q_\mu(k_x, k_y, k_z) \equiv q_\mu \sum_{l_x=-\infty}^{l_x=\infty}\sum_{l_y=-\infty}^{l_y=\infty}\sum_{l_z=-\infty}^{l_z=\infty} M_n\left(\frac{x_\mu}{\Delta x} - k_x + l_x K_x\right) \times M_n\left(\frac{y_\mu}{\Delta y} - k_y + l_y K_y\right) M_n\left(\frac{z_\mu}{\Delta z} - k_z + l_z K_z\right). \tag{A12}$$

Here, $\alpha_\mu(\alpha = x, y, z)$ is the α-component of the position of atom μ, and $M_n(x)$ is the nth cardinal B-spline function, defined recursively as

$$M_2(x) \equiv \begin{cases} 1 - |x - 1|, & 0 \le x \le 2, \\ 0, & \text{otherwise}, \end{cases} \tag{A13}$$

$$M_n(x) \equiv \frac{x}{n-1} M_{n-1}(x) + \frac{n-x}{n-1} M_{n-1}(x-1). \tag{A14}$$

Sakuraba *et al.* derived the following expression of $u_{\mathrm{recp},i}$ from the linearity of the Fourier transform:

$$u_{\mathrm{recp},i} = \sum_{k_x=0}^{K_x-1} \sum_{k_y=0}^{K_y-1} \sum_{k_z=0}^{K_z-1} \mathcal{F}^{-1}\left[\mathcal{D} \cdot \mathcal{F}\left[\sum_{\mu \in u} Q_\mu\right]\right] \sum_{\nu \in i} Q_\nu(k_x, k_y, k_z), \tag{A15}$$

where $\mathcal{D}(m_x, m_y, m_z)$ is reciprocal-space function defined as

$$\mathcal{D}(m_x, m_y, m_z) \equiv \begin{cases} 0, & (m_x, m_y, m_z) = 0 \\ \dfrac{1}{\pi V \gamma(m_x, m_y, m_z)} \dfrac{\exp\left[-\pi^2 |\boldsymbol{g}|^2 / \kappa^2\right]}{|\boldsymbol{g}|^2} & \text{otherwise.} \end{cases} \tag{A16}$$

In the above equation, $\gamma(m_x, m_y, m_z)$ is a normalization factor given by

$$\gamma(m_x, m_y, m_z) \equiv \prod_{\alpha=x,y,z} \left| \sum_{l=0}^{n-2} M_n(l+1) \exp\left[-\frac{2\pi \imath m_i}{K_\alpha}\right] \right|^2, \tag{A17}$$

and $\boldsymbol{g}$ is a three-dimensional vector defined as

$$\boldsymbol{g} \equiv \left(\frac{m'_x}{L_x}, \frac{m'_y}{L_y}, \frac{m'_z}{L_z}\right), \tag{A18}$$

and $m'_\alpha \equiv m_\alpha$ for $0 \le m_\alpha \le K_\alpha/2$ and $m'_\alpha \equiv m_\alpha - K_\alpha$ otherwise.

The pair force acting on ith solvent can be evaluated from the derivative of the pair interaction with respect to the positions of atoms in the molecule. It is straightforward to perform the derivatives of $u_{\mathrm{LJ},i}$ [Eq. (A2)] and $u^{(s)}_{\mathrm{elec},i}$ [Eq. (A5)], and the resultant expressions are

$$\boldsymbol{f}_{\mathrm{LJ},i} \equiv \sum_{\mu \in u} \sum_{\nu \in i} 4\varepsilon_{\mu\nu} \left[12 \left(\frac{\sigma_{\mu\nu}}{r_{\mu\nu}}\right)^{12} - 6 \left(\frac{\sigma_{\mu\nu}}{r_{\mu\nu}}\right)^{6} \right] \frac{\boldsymbol{r}_\nu - \boldsymbol{r}_\mu}{r^2_{\mu\nu}}, \tag{A19}$$

$$\boldsymbol{f}^{(s)}_{\mathrm{elec},i} \equiv \sum_{\mu \in u} \sum_{\nu \in i} q_\mu q_\nu \left[\frac{1 - \mathrm{erf}(\kappa r_{\mu\nu})}{r_{\mu\nu}} + \frac{2\kappa}{\sqrt{\pi}} \exp\left[-\kappa^2 r^2_{\mu\nu}\right] \right] \frac{\boldsymbol{r}_\nu - \boldsymbol{r}_\mu}{r^2_{\mu\nu}}. \tag{A20}$$

From Eqs. (A7) and (A8), the pair force, which stems from $u^{(l)}_{\mathrm{elec},i}$, $\boldsymbol{f}^{(l)}_{\mathrm{elec},i}$, is described as

$$\boldsymbol{f}^{(l)}_{\mathrm{elec},i} = -\sum_{\nu \in i} \frac{\partial u_{\mathrm{recp},i}}{\partial \boldsymbol{r}_\nu}. \tag{A21}$$

In Eq. (A15), only $Q_\nu(k_x, k_y, k_z)$ $(\nu \in i)$ depends on the solvent atom position, and hence

$$\boldsymbol{f}^{(l)}_{\mathrm{elec},i} = -\sum_{k_x=0}^{K_x-1} \sum_{k_y=0}^{K_y-1} \sum_{k_z=0}^{K_z-1} \mathcal{F}^{-1}\left[\mathcal{D} \cdot \mathcal{F}\left[\sum_{\mu \in u} Q_\mu\right]\right] \sum_{\nu \in i} \frac{\partial Q_\nu(k_x, k_y, k_z)}{\partial \boldsymbol{r}_\nu}. \tag{A22}$$

Utilizing the following relationship:

$$\frac{\mathrm{d}\, M_n(x)}{\mathrm{d}x} = M_{n-1}(x) - M_{n-1}(x-1), \tag{A23}$$

α-component of $\partial Q_\nu / \partial \boldsymbol{r}_\nu$ can be written as

$$\begin{aligned} \frac{\partial Q_\nu(k_x, k_y, k_z)}{\partial \alpha_\nu} = q_\mu \sum_{l_x=-\infty}^{l_x=\infty} \sum_{l_y=-\infty}^{l_y=\infty} \sum_{l_z=-\infty}^{l_z=\infty} \left[\prod_{\beta \neq \alpha} M_n\left(\frac{\beta_\mu}{\Delta\beta} - k_\beta + l_\beta K_\beta\right) \right] \\ \times \left[M_{n-1}\left(\frac{\alpha_\mu}{\Delta\alpha} - k_\alpha + l_\alpha K_\alpha\right) \right. \\ \left. - M_{n-1}\left(\frac{\alpha_\mu}{\Delta\alpha} - k_\alpha + l_\alpha K_\alpha - 1\right) \right] \frac{1}{\Delta\alpha}. \end{aligned} \tag{A24}$$

The total pair force acting on ith solvent molecule, $\boldsymbol{f}^G_i$, is

$$\boldsymbol{f}^G_i = \boldsymbol{f}_{\mathrm{LJ},i} + \boldsymbol{f}^{(s)}_{\mathrm{elec},i} + \boldsymbol{f}^{(l)}_{\mathrm{elec},i}. \tag{A25}$$

Owing to the action-reaction law of Newtonian mechanics, the force acting on the solute molecule from ith solvent molecule, $\boldsymbol{F}_{u \leftarrow i}$, is readily obtained as

$$\boldsymbol{F}_{u \leftarrow i} = -\boldsymbol{f}^G_i. \tag{A26}$$

REFERENCES

[1] J. R. Lakowicz, *Principles of Fluorescence Spectroscopy* (Springer, 2006).
[2] I. L. Medintz and N. Hildebrandt, *FRET-förster Resonance Energy Transfer: From Theory to Applications* (John Wiley and Sons, 2013).
[3] M. Maroncelli, J. Mol. Liq. **57**, 1 (1993).
[4] A. Nitzan, *Chemical Dynamics in Condensed Phases: Relaxation, Transfer and Reactions in Condensed Molecular Systems* (Oxford University Press, 2006).
[5] B. Bagchi, *Molecular Relaxation in Liquids* (OUP, 2012).

[6]G. Gunther, L. Malacrida, D. M. Jameson, E. Gratton, and S. A. Sánchez, Acc. Chem. Res. **54**, 976 (2021).
[7]S. Osella and S. Knippenberg, Biochim. Biophys. Acta, Biomembr. **1863**, 183494 (2021).
[8]S. A. Rice, *Diffusion-limited Reactions* (Elsevier, 1985), Vol. 25.
[9]N. Pottier, *Nonequilibrium Statistical Physics: Linear Irreversible Processes* (Oxford University Press, 2009).
[10]K. Lindenberg, R. Metzler, and G. Oshanin, *Chemical Kinetics: Beyond the Textbook* (World Scientific, 2019).
[11]D. F. Calef and P. G. Wolynes, J. Chem. Phys. **78**, 4145 (1983).
[12]A. Chandra and B. Bagchi, Chem. Phys. Lett. **151**, 47 (1988).
[13]A. Chandra and B. Bagchi, J. Chem. Phys. **94**, 8367 (1991).
[14]S. Egorov, Phys. Rev. Lett. **93**, 023004 (2004).
[15]R. Schilling and T. Scheidsteger, Phys. Rev. E **56**, 2932 (1997).
[16]L. Fabbian, A. Latz, R. Schilling, F. Sciortino, P. Tartaglia, and C. Theis, Phys. Rev. E **60**, 5768 (1999).
[17]T. Theenhaus, R. Schilling, A. Latz, and M. Letz, Phys. Rev. E **64**, 051505 (2001).
[18]F. Hirata, *Molecular Theory of Solvation*, Vol. 24 (Springer Science & Business Media, 2003).
[19]K. Kasahara and H. Sato, Phys. Chem. Chem. Phys. **19**, 27917 (2017).
[20]D. Chandler and H. C. Andersen, J. Chem. Phys. **57**, 1930 (1972).
[21]F. Hirata and P. J. Rossky, Chem. Phys. Lett. **83**, 329 (1981).
[22]F. Hirata, P. J. Rossky, and B. M. Pettitt, J. Chem. Phys. **78**, 4133 (1983).
[23]J. P. Hansen and I. R. McDonald, *Theory of Simple Liquids* (Academic Press, London, 2013).
[24]H. Mori, Prog. Theor. Phys. **33**, 423 (1965).
[25]R. Zwanzig, *Nonequilibrium Statistical Mechanics* (Oxford University Press, 2001).
[26]U. Balucani and M. Zoppi, *Dynamics of the Liquid State*, Vol. 10 (Clarendon Press, 1995).
[27]F. O. Raineri, Y. Zhou, H. L. Friedman, and G. Stell, Chem. Phys. **152**, 201 (1991).
[28]F. Hirata, J. Chem. Phys. **96**, 4619 (1992).
[29]S.-H. Chong and F. Hirata, Phys. Rev. E **58**, 6188 (1998).
[30]S.-H. Chong and F. Hirata, J. Chem. Phys. **111**, 3654 (1999).
[31]S.-H. Chong and W. Götze, Phys. Rev. E **65**, 051201 (2002).
[32]T. Yamaguchi and F. Hirata, J. Chem. Phys. **117**, 2216 (2002).
[33]S.-H. Chong and F. Hirata, J. Chem. Phys. **111**, 3083 (1999).
[34]T. Yamaguchi, S.-H. Chong, and F. Hirata, J. Chem. Phys. **119**, 1021 (2003).
[35]T. Yamaguchi, S.-H. Chong, and F. Hirata, J. Mol. Liq. **112**, 117 (2004).
[36]A. E. Kobryn, T. Yamaguchi, and F. Hirata, J. Mol. Liq. **119**, 7 (2005).
[37]S.-H. Chong and F. Hirata, J. Chem. Phys. **108**, 7339 (1998).
[38]T. Yamaguchi, T. Matsuoka, and S. Koda, J. Chem. Phys. **127**, 234501 (2007).
[39]T. Yamaguchi, T. Matsuoka, and S. Koda, J. Chem. Phys. **126**, 144505 (2007).
[40]A. E. Kobryn and F. Hirata, J. Chem. Phys. **126**, 044504 (2007).
[41]F. Hirata, T. Munakata, F. Raineri, and H. L. Friedman, J. Mol. Liq. **65–66**, 15 (1995).
[42]F. O. Raineri, B.-C. Perng, and H. L. Friedman, Chem. Phys. **183**, 187 (1994).
[43]H. L. Friedman, F. O. Raineri, F. Hirata, and B.-C. Perng, J. Stat. Phys. **78**, 239 (1995).
[44]T. Ishida, F. Hirata, and S. Kato, J. Chem. Phys. **110**, 11423 (1999).
[45]K. Nishiyama, F. Hirata, and T. Okada, J. Mol. Struct. **565–566**, 31 (2001).
[46]K. Nishiyama, F. Hirata, and T. Okada, J. Chem. Phys. **118**, 2279 (2003).
[47]K. Nishiyama, T. Yamaguchi, and F. Hirata, J. Phys. Chem. B **113**, 2800 (2009).
[48]D. Beglov and B. Roux, J. Phys. Chem. B **101**, 7821 (1997).
[49]A. Kovalenko and F. Hirata, Chem. Phys. Lett. **290**, 237 (1998).
[50]A. Kovalenko and F. Hirata, J. Chem. Phys. **110**, 10095 (1999).
[51]A. Yoshimori, J. Theor. Comput. Chem. **03**, 117 (2004).
[52]K. Kasahara and H. Sato, J. Chem. Phys. **140**, 244110 (2014).
[53]A. Yoshimori, J. Phys. Soc. Jpn. **80**, 034801 (2011).
[54]T. Yamaguchi and N. Yoshida, J. Chem. Phys. **154**, 044504 (2021).
[55]N. Matubayasi and M. Nakahara, J. Chem. Phys. **113**, 6070 (2000).
[56]N. Matubayasi and M. Nakahara, J. Chem. Phys. **117**, 3605 (2002).
[57]N. Matubayasi and M. Nakahara, J. Chem. Phys. **119**, 9686 (2003).
[58]S. Sakuraba and N. Matubayasi, J. Comput. Chem. **35**, 1592 (2014).
[59]A. I. Frolov, J. Chem. Theory Comput. **11**, 2245 (2015).
[60]N. Matubayasi, Bull. Chem. Soc. Jpn. **92**, 1910 (2019).
[61]R. Urano, G. A. Pantelopulos, and J. E. Straub, J. Phys. Chem. B **123**, 2546 (2019).
[62]N. Matubayasi, W. Shinoda, and M. Nakahara, J. Chem. Phys. **128**, 195107 (2008).
[63]T. Mizuguchi and N. Matubayasi, J. Phys. Chem. B **122**, 3219 (2018).
[64]K. Kasahara, R. Masayama, K. Okita, and N. Matubayasi, J. Chem. Phys. **155**, 204503 (2021).
[65]K. Kasahara and H. Sato, J. Chem. Phys. **145**, 194502 (2016).
[66]E. Fick, G. Sauermann, and W. D. Brewer, *The Quantum Statistics of Dynamic Processes* (Springer, 1990), Vol. 86.
[67]T. Koide, Phys. Rev. E **72**, 026135 (2005).
[68]K.-M. Tu, R. Ishizuka, and N. Matubayasi, J. Chem. Phys. **141**, 244507 (2014).
[69]R. A. Marcus, Annu. Rev. Phys. Chem. **15**, 155 (1964).
[70]E. A. Carter and J. T. Hynes, J. Phys. Chem. **93**, 2184 (1989).
[71]T. Yamaguchi, T. Matsuoka, and S. Koda, J. Chem. Phys. **123**, 034504 (2005).
[72]B. B. Laird and W. H. Thompson, J. Chem. Phys. **126**, 211104 (2007).
[73]M. Frisch, G. Trucks, H. Schlegel, G. Scuseria, M. Robb, J. Cheeseman, G. Scalmani, V. Barone, G. Petersson, H. Nakatsuji *et al.*, GAUSSIAN 16, Gaussian, Inc., 2016.
[74]J. Wang, R. M. Wolf, J. W. Caldwell, P. A. Kollman, and D. A. Case, J. Comput. Chem. **25**, 1157 (2004).
[75]L. Martínez, R. Andrade, E. G. Birgin, and J. M. Martínez, J. Comput. Chem. **30**, 2157 (2009).
[76]W. C. Swope, H. C. Andersen, P. H. Berens, and K. R. Wilson, J. Chem. Phys. **76**, 637 (1982).
[77]G. Bussi, D. Donadio, and M. Parrinello, J. Chem. Phys. **126**, 014101 (2007).
[78]S. Miyamoto and P. A. Kollman, J. Comput. Chem. **13**, 952 (1992).
[79]J. Jung, T. Mori, C. Kobayashi, Y. Matsunaga, T. Yoda, M. Feig, and Y. Sugita, Wiley Interdiscip. Rev.: Comput. Mol. Sci. **5**, 310 (2015).
[80]C. Kobayashi, J. Jung, Y. Matsunaga, T. Mori, T. Ando, K. Tamura, M. Kamiya, and Y. Sugita, J. Comput. Chem. **38**, 2193 (2017).
[81]J. Jung, C. Kobayashi, K. Kasahara, C. Tan, A. Kuroda, K. Minami, S. Ishiduki, T. Nishiki, H. Inoue, Y. Ishikawa, M. Feig, and Y. Sugita, J. Comput. Chem. **42**, 231 (2021).
[82]W. Humphrey, A. Dalke, and K. Schulten, J. Mol. Graph. **14**, 33 (1996).
[83]J. H. Ferziger, M. Perić, and R. L. Street, *Computational Methods for Fluid Dynamics* (Springer, 2002), Vol. 3.
[84]K. Kasahara and H. Sato, J. Comput. Chem. **39**, 1491 (2018).
[85]Schrödinger, LLC, The PyMOL molecular graphics system, version 2.5.2, 2021.
[86]S. W. Lovesey, J. Phys. C: Solid State Phys. **4**, 3057 (1971).
[87]J. R. D. Copley and S. W. Lovesey, Rep. Prog. Phys. **38**, 461 (1975).
[88]L. Sjögren, Phys. Rev. A **22**, 2866 (1980).
[89]L. Sjögren, Phys. Rev. A **22**, 2883 (1980).
[90]L. Sjögren, J. Phys. C: Solid State Phys. **13**, 705 (1980).
[91]U. Essmann, L. Perera, M. L. Berkowitz, T. Darden, H. Lee, and L. G. Pedersen, J. Chem. Phys. **103**, 8577 (1995).